

See discussions, stats, and author profiles for this publication at: <https://www.researchgate.net/publication/322599294>

Improving high power properties of PZT ceramics by external DC bias field

Article in *Journal of the American Ceramic Society* · January 2018

DOI: 10.1111/jace.15437

CITATIONS

0

READS

130

6 authors, including:



[Anushka Bansal](#)

Pennsylvania State University

10 PUBLICATIONS 62 CITATIONS

[SEE PROFILE](#)



[Kenji Uchino](#)

Pennsylvania State University

525 PUBLICATIONS 17,353 CITATIONS

[SEE PROFILE](#)

Some of the authors of this publication are also working on these related projects:



High Power Piezoelectric Characterization & Loss Mechanisms [View project](#)



Ferroelectrics [View project](#)

All content following this page was uploaded by [Kenji Uchino](#) on 22 February 2018.

The user has requested enhancement of the downloaded file.

ORIGINAL ARTICLE

Improving high-power properties of PZT ceramics by external DC bias field

Anushka Bansal¹  | Husain N. Shekhani² | Maryam Majzoubi¹ | Eberhard Hennig³ | Timo Scholehwar³ | Kenji Uchino¹¹International Center for Actuators and Transducers, The Pennsylvania State University, State College, Pennsylvania²Kulicke & Soffa Industries, Santa Ana, California³R&D Department, PI Ceramic GmbH, Lederhose, Germany

Correspondence

Anushka Bansal, International Center for Actuators and Transducers, The Pennsylvania State University, State College, PA.

Email: anushka.4353.bansal@gmail.com

Funding information

Office of Naval Research Global, Grant/Award Number: N00014-14-1-1044

Abstract

This paper concludes that the deterioration of the mechanical quality factor Q_m when operated under high power, can be recovered by externally applying positive DC bias field. Material constants for piezoelectric ceramics are generally characterized under low-power conditions. However, high-power properties deviate significantly from the ones measured under low-power conditions (Q_m degrades by a factor of ~ 2). DC Bias field helps to recover the properties of the ceramic under high-power conditions. The DC bias field of 200 V/mm exhibits an almost equivalent “opposite” change rate to the vibration velocity of 0.1 m/s. It is also notable that the piezoelectric loss $\tan \theta'$ can be decreased most effectively under positive DC bias field (1.9% per 100 V/mm for the hard PZT and 3.1% per 100 V/mm for the soft PZT), in comparison with the elastic or dielectric losses. This report presents a comprehensive analysis on the low- and high-power piezoelectric properties of hard and soft Lead Zirconate Titanates (PZT's) under externally applied DC bias field in the k_{31} resonance mode (transverse extensional).

KEYWORDS

burst drive method, continuous admittance spectrum, DC bias field, high power, losses in piezoelectrics, vibration velocity

1 | INTRODUCTION

Piezoelectric materials such as Lead-Zirconate Titanates [$\text{Pb}(\text{Zr}_x\text{Ti}_{1-x})\text{O}_3$, PZT's] have been widely adopted for many applications such as underwater sonars, motors, and piezoelectric transformers.¹⁻³ To miniaturize the piezoelectric actuators and transducers, high-power-density piezoelectric material developments are required to realize the same level of mechanical vibration energy in a smaller specimen, without temperature rise through internal losses. High-power characterization of a piezoelectric element under a high vibration velocity exhibits, in general, significant nonlinearity in the dielectric, elastic and piezoelectric performances, as well as the corresponding loss tangents and heat generation⁴⁻⁶ Although material constants for piezoelectric ceramics are generally characterized under

free or unloaded conditions, these measured properties are not valid directly when devices work under externally applied mechanical or electrical loads. Therefore, an important topic of investigation currently is the behavior of the loss mechanisms under different conditions. DC bias stress and electric field are of particular importance for study because the actuators and transducers are often used in these circumstances to stabilize or enhance the operation performance.⁷ So-called bolt-clamped Langevin transducers provided enhancement in the transducer characteristics, which is related to the external preload stress.^{8,9}

Regarding the bias electric field effect, previous reports¹⁰⁻¹² clarified the stabilization mechanism of the high-power performance in “Hard” $\text{Pb}(\text{Zr},\text{Ti})\text{O}_3$ (PZT)-based ceramics in terms of the “internal” bias field. As shown in Figure 1A, the mechanical quality factor Q_m in

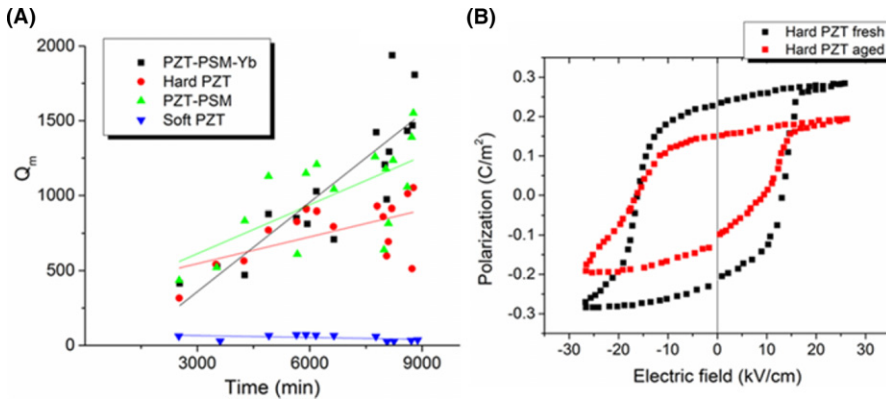


FIGURE 1 Q_m as a function of time for various hard and soft PZT's, measured after fresh electric poling; (B) Hysteresis curve shape change with time, showing the internal bias field generation in the hard PZT. (Cited from Ref. 12)

the hard PZT increases rather gradually after the electric poling process (~ 2 hours) to reach to the value higher than 1000, whereas the soft PZT does not change the Q_m value with time lapse. Also, the polarization versus electric field hysteresis curve change with the time lapse, where the internal “positive” electric field is created in an “aged” sample (Figure 1B).¹⁰ Accordingly, we proposed that the high Q_m is primarily triggered by the “internal” bias field, which may be attributed to the defect dipoles originated from a slow rate of oxygen ion diffusion after the poling.¹² To further explore the loss mechanism in PZT's, instead of the “internal” bias field in hard PZT, we studied the “external” bias field effect in both hard and soft PZT's in this paper. Although there are several papers already reported including ours,^{13,14} the previous papers have not measured detailed data in three loss behaviors separately.

This paper mainly focuses on the dependence of properties of the PZT k_{31} -type plates under different vibration velocity conditions as a function of external DC bias field, by comparing the results among hard and soft PZT's. The goal of this paper is to clarify the DC bias field dependence of three losses (dielectric, elastic and piezoelectric losses), which are primarily caused by semimicroscopic domain dynamics.

2 | EXPERIMENTAL PROCEDURES

We used PIC 144 and PIC 255 as hard and soft PZT's, respectively, in this study. These PZT ceramic plates were prepared in the R&D Department, PI Ceramic GmbH (Lindenstrasse, 07589 Lederhose, Germany). All the plate samples (5 pieces for each with the smallest deviation in properties especially losses) with the size of 40 mm long \times 5 mm wide \times 0.5 mm thick were silver-electroded on 40 mm \times 5 mm face, and electrically poled at 70°C for 7 hours and 1 hour, respectively, for hard and soft PZT's along the thickness direction. The ICAT experimental setup, High Power Characterization System (HiPoCS)¹⁵ was used to carry out the experiments.^{16,17}

To escape from the temperature effect, high-power measurements were performed using the burst method¹⁸⁻²³ whereas, low-power measurements were performed by continuous admittance spectrum method. Electrical spectroscopy method being a continuous drive method, better represents the driving conditions of an actual device, and therefore may provide the most significant data for transducer design. However, in high-power conditions significant heat is generated, causing temperature rise and temperature distribution in the sample. As a result, it is not possible to separate the effects of temperature rise and property changes in the continuous method using procedures outlined in the literature. Therefore, the advantage of the burst method is that temperature rise is not excited due to low driving times (often less than 10 ms). This allows for the characterization of the high-power behavior as function of vibration and as a function of the temperature of the testing environment. It is noteworthy that RMS edge vibration velocity is used in the discussion of this paper. In parallel, the permittivity ϵ_{33}^T was measured at 1 kHz (off-resonance) by an LCR meter [SR715, Stanford Research Systems, Inc., Sunnyvale, CA]. Also, DC bias field was applied using an external amplifier. In this paper, the bias field direction is denoted “positive” when the field is applied along the polarization direction. The external DC bias field applied to the sample was varied from -160 to $+320$ V/mm. The standard deviation is indicated by a short vertical bar on each measured data point in all figure, estimated from 5 samples and 5 cyclical measurements.

Figure 2 shows the polarization versus electric field hysteresis curves at 10 Hz for hard (PIC 144) and soft (PIC 255) PZT's (roughly 10 weeks aged). In comparison with a symmetric curve for the soft PZT, we observed a positively biased hysteresis ($E_{\text{bias}} \approx 700$ V/mm) curve in the hard PZT sample which verified the earlier argument about internal DC bias field already present in the hard PZT piezoelectric ceramics. The derivative of the P - E curve provides permittivity at a low frequency of 10 Hz, which is inserted in Figure 4 and discussed later.

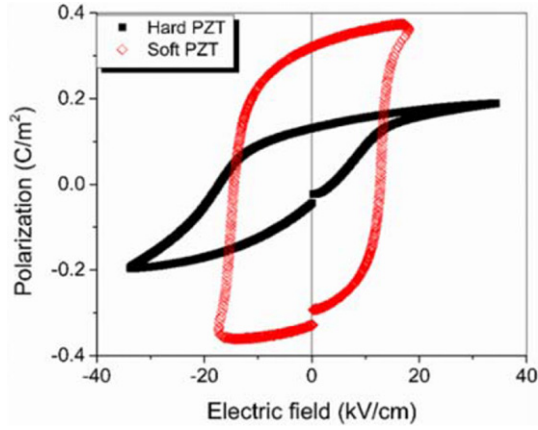


FIGURE 2 P-E hysteresis loop for hard and soft PZT's

3 | LOSS CHARACTERIZATION PHENOMENOLOGY

Losses in piezoelectric materials originate from three different properties: dielectric, elastic, and piezoelectric. Intensive dielectric, elastic, and piezoelectric losses are defined by

$$\varepsilon^{T*} = \varepsilon^T (1 - j \tan \delta')$$
 (1)

$$s^{E*} = s^E (1 - j \tan \phi')$$
 (2)

$$d^* = d (1 - j \tan \theta')$$
 (3)

Here j is the imaginary notation, ε^T the dielectric constant under constant stress (intensive parameter), s^E the elastic compliance under constant electric field (intensive parameter), and d the piezoelectric constant. The loss tangent value should be much smaller than 1 (less than 0.1 in practice) in this complex parameter usage and means a phase/time lag of the output parameter (such as P) from the input parameter (such as E). It becomes very important here to have an understanding here of what do we mean by intensive properties. The material property relationships that are governed by externally controlled parameters are called intensive material properties, and those properties that are governed by indirectly controlled parameters are called extensive material properties. The terms extensive and intensive were coined to avoid confusion with intrinsic (unit cell) and extrinsic (domain wall related) contributions to piezoelectric properties.

Intensive loss components of these three can be obtained from the resonance and anti-resonance mechanical quality factors Q_A and Q_B in the k_{31} mode from the following equations (Equations 4-8) proposed in our previous papers.^{13,18}

$$Q_{A,31} = \frac{1}{\tan \phi'_{11}} \quad (4)$$

$$\frac{1}{Q_{B,31}} = \frac{1}{Q_{A,31}} + \frac{2}{1 + \left(\frac{1}{k_{31}} - k_{31}\right)^2 \Omega_{B,31}^2} \quad (5)$$

$$(\tan \delta'_{33} + \tan \phi'_{11} - 2 \tan \theta'_{31})$$

Here k_{31} is the electromechanical coupling factor, $\tan \delta'_{33}$, $\tan \phi'_{11}$, $\tan \theta'_{31}$ are intensive loss factors for ε_{33}^T , s_{11}^E , d_{31} , respectively. The parameter $\Omega_{B,31}$ is proportional to the antiresonance frequency ω_B (Equation 6):

$$\Omega_{B,31} = \frac{\omega_B L}{2v_{11}^E} \quad (6)$$

where v_{11}^E is the sound velocity of the material in the direction of length L and ρ is the density and is given by $v_{11}^E = \frac{1}{\sqrt{\rho s_{11}^E}}$.

The elastic compliance s_{11}^E can be calculated from the resonance frequency as

$$s_{11}^E = \frac{1}{(2Lf_A)^2 \rho} \quad (7)$$

The electromechanical coupling factor k_{31} is defined by the following equation:

$$k_{31}^2 = \frac{d_{31}^2}{s_{11}^E (\varepsilon_{33}^T \varepsilon_0)} \quad (8)$$

where d_{31} is the piezoelectric constant, s_{11}^E is the elastic compliance at a constant electric field, ε_{33}^T is the free (unclamped) permittivity, ε_0 is the permittivity under vacuum. Electromechanical coupling factor k_{31} can be calculated from the resonance and antiresonance frequencies as

$$k_{31}^2 = \frac{\frac{\pi f_B}{2f_A} \cdot \tan\left(\frac{\pi f_B - f_A}{2f_A}\right)}{1 + \frac{\pi f_B}{2f_A} \cdot \tan\left(\frac{\pi f_B - f_A}{2f_A}\right)} \quad (9)$$

Now, to obtain $\tan \phi'$, Q_A is measured, and inverse value gives elastic loss. Then, knowing $\tan \delta'$ from the LCR meter at the off-resonance frequency, evaluating Q_B , we can calculate $\tan \theta'$ using Equations (5) and (6).

4 | HIGH-POWER MEASUREMENTS WITHOUT APPLYING EXTERNAL DC BIAS FIELD

Initially, high-power measurements were conducted without applying external DC bias field. The material's parameters were obtained using the burst/transient method.¹⁵ In the burst mode, the ceramic is electrically driven at its resonance (or antiresonance) frequency for a small number of cycles to excite the mechanical vibration with the desired vibration velocity. Because of the short period excitation (less than

1 ms), practical temperature rise does not occur in the sample (less than 0.02°C) even under a high vibration excitation. Then, either a short or open circuit condition is imposed after removing or isolating the excitation electric power. When the sample oscillates at the resonance frequency and the short-circuit condition is imposed, rendered current is proportional to the vibration velocity (i.e., the ratio provides Force Factor A). Whereas, when an open-circuit condition is imposed, generated voltage is proportional to the vibration displacement (the ratio provides Voltage Factor B), and the oscillation frequency is the antiresonance frequency.

By measuring the rate of signal decay, the quality factor can be measured using the relative rate of decay of vibration amplitude for a damped linear system oscillating at its natural frequency using Equation (10)

$$Q = \frac{2\pi f}{\frac{2\ln(v_1/v_2)}{(t_2-t_1)}} \quad (10)$$

where f is the natural mechanical resonance frequency (i.e., resonance or antiresonance frequency, depending on the electrical boundary condition). Here v_1 and v_2 are vibration velocity at two different decay time, t_1 and t_2 (typically with $t_2 - t_1 =$ difference between two measured vibration cycles after removing or isolating the excitation power to obtain Q at an excited vibration velocity). Very short measuring time (~5 seconds) required for obtaining full physical parameters (via LabView software) as a function of vibration velocity under the short- or open-circuit condition is an additional attractive point in the burst mode method.

We summarize here how to determine the “real” parameters, dielectric permittivity, elastic compliance and piezoelectric constant from the burst method in the case of a k_{31} plate as illustrated in Figure 3. Here, L is the length, b , the width and a is the height of the PZT ceramic plate. The force factor A_{31} is calculated as the ratio of the short-circuit current i_0 over the vibration velocity v_0 at the plate length edge in the resonance, and is given by Equation (11).

$$A_{31} = \frac{i_0}{v_0} = -2b \frac{d_{31}}{s_{11}^E} \quad (11)$$

It is notable that $\left(\frac{d_{31}}{s_{11}^E}\right)$ is not equal to the off-resonance piezoelectric stress coefficient e_{31} , but e_{31}^* in our previous paper because of only longitudinally excited resonance ($X_2 = X_3 = 0$).¹⁵

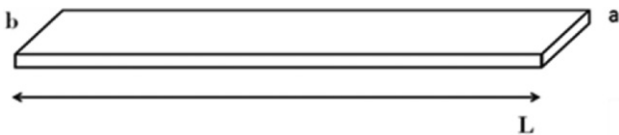


FIGURE 3 A rectangular PZT plate with all the dimensions marked (L: length, b: width, a: thickness)

While, the voltage factor B_{31} is the relationship between the open-circuit voltage and displacement at the plate length edge at the antiresonance, expressed by Equation (12).

$$B_{31} = \frac{V_0}{u_0} = \frac{2a}{L} \frac{d_{31}}{s_{11}^E \epsilon_0 \epsilon_{33}^x} \quad (12)$$

On similar lines, $\frac{d_{31}}{s_{11}^E \epsilon_0 \epsilon_{33}^x}$ is not exactly equal to the converse piezoelectric coefficient h_{31} .¹⁵

It is important to note that we can obtain longitudinally clamped permittivity $\epsilon_{33}^x \epsilon_0$ (longitudinally clamped or effective damped permittivity) even at the resonance-antiresonance frequency range from the ratio of the force factor A_{31} over the voltage factor B_{31} in the following formula:

$$\epsilon_0 \epsilon_{33}^x (1 - k_{31}^2) = \epsilon_0 \epsilon_{33}^x = \frac{|A_{31}| a}{B_{31} L b} \quad (13)$$

Thus, free permittivity ϵ_{33}^x can be calculated from the relationship with the electromechanical coupling factor k_{31} . The determination of the permittivity at the resonance frequency is another attractive point of the burst method. Note that the burst mode measurement is not associated with heat generation (temperature rise can be estimated less than 0.02°C) even under very high vibration velocity.

5 | ELASTIC COMPLIANCE

Figure 4A shows the elastic compliance change with the vibration velocity calculated from the resonance frequency (from Equation (7)), measured for the hard (PIC 144) and soft (PIC 255) PZT's. Both samples exhibit a nearly linear compliance increase, where the change rate (3% per 0.1 m/s) for the hard PZT is less than the rate (5% per 0.1 m/s) for the soft PZT.

Taking the inverse value of Q_A (Figure S1), the elastic loss $\tan \phi'$ change is plotted in Figure 5A, where the vertical axis scale differs 100 times between the hard and soft PZT's. Although both samples exhibit the elastic loss increase, the change rate of the soft PZT is rather monotonous (75% per 0.1 m/s). On the contrary, the change in the hard PZT seems to be a two-step process: almost constant up to 0.13 m/s, and followed by the rate of 75% per 0.1 m/s, a similar rate to the soft PZT. There appears to be a threshold vibration velocity in the hard PZT, below which the subcoercive domain wall switching may not happen significantly.

6 | DIELECTRIC PERMITTIVITY

The dielectric permittivity at high-power conditions was determined from Equations (12) and (13). Figure 4B shows longitudinally clamped (or effective damped) permittivity ϵ_{33}^x and free permittivity ϵ_{33}^T (calculated from the relation

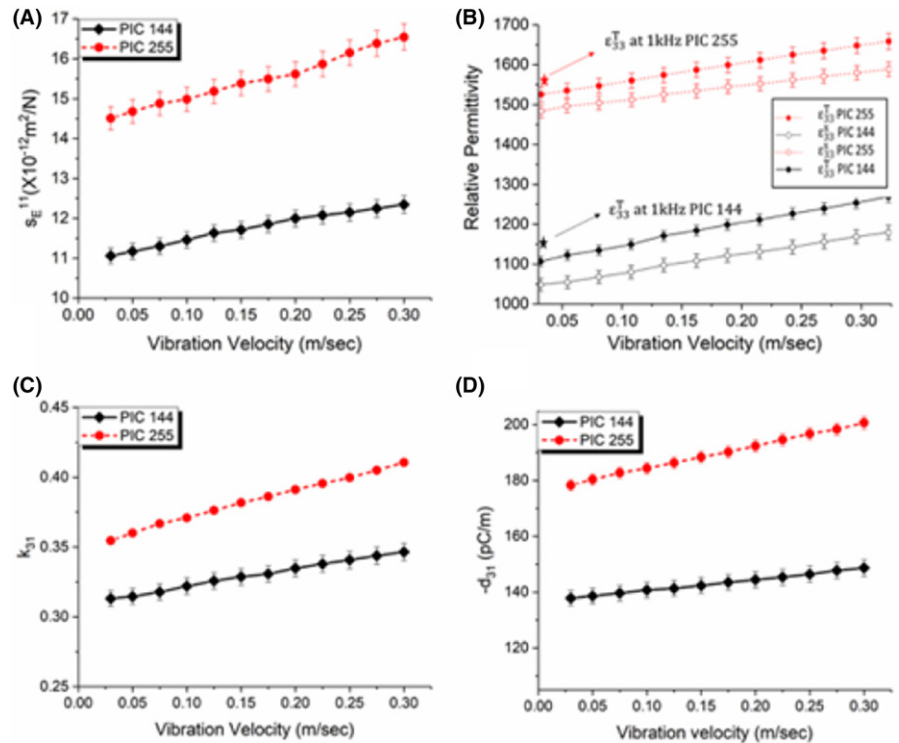


FIGURE 4 Real parameters under zero DC bias (A) Elastic compliance (B) Relative Permittivity (C) Electromechanical coupling factor (D) Piezoelectric constant for PIC 144 (hard PZT) and PIC 255 (soft PZT). The real parameters increased as a function of vibration velocity

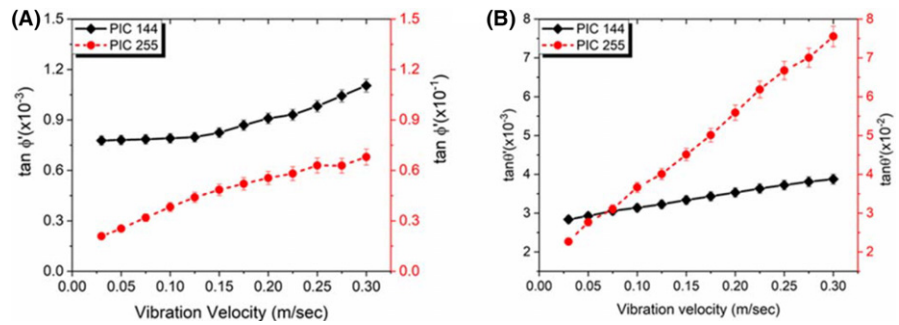


FIGURE 5 Losses under zero DC bias (A) Elastic loss (B) Piezoelectric loss for PIC 144 (hard PZT) and PIC 255 (soft PZT). The losses increased as a function of vibration velocity indicating heat generation in the ceramic under high-power conditions

$\epsilon_{33}^x = \epsilon_{33}^T = (1 - k_{31}^2)$ with the k_{31} value obtained in the next section) as a function of vibration velocity for the both soft and hard PZT's. For comparison, ϵ_{33}^T measured at 1 kHz (off-resonance) by LCR meter is also plotted. It was observed that the calculated permittivity ϵ_{33}^T at the resonance (high frequency) is slightly lower than the one at the off-resonance 1 kHz, which is probably related to the general frequency dependence of the permittivity, supported by the ϵ_{33}^T values of 1230 (Hard) and 1610 (Soft) at 10 Hz in Figure 7. It is noteworthy that the clamped permittivity ϵ_{33}^x also shows the increase with an increase in vibration velocity, which may be explained by the fact that this “clamp” does not mean complete clamp, but just 1D longitudinal clamp. However, since we have not established the method yet for obtaining the dielectric loss at the resonance frequency, this paper adopts $\tan \delta = 0.002$ and 0.027 at the off-resonance (1 kHz) for the hard and soft PZT's, respectively, for the loss analysis described below.

7 | PIEZOELECTRIC CONSTANT AND ELECTROMECHANICAL COUPLING FACTOR

Figure 4C,D shows the electromechanical coupling factor k_{31} and piezoelectric constant d_{31} change with vibration velocity for the hard and soft PZT's using Equation s (8) and (9). The electromechanical coupling factor for both samples increased, the change rate (3.5% per 0.1 m/s) for the hard PZT is less than the rate (5.3% per 0.1 m/s) for the soft PZT. Also, the piezoelectric constant increased with increasing vibration velocity. The change rate was lower for the hard PZT (2.7% per 0.1 m/s) than the soft PZT (5.1% per 0.1 m/s).

The intensive piezoelectric loss was determined from the mechanical quality factors Q_A and Q_B with the help of Equation (5) and plotted in Figure 5B. Note the vertical scale difference of 10 times between the hard and soft PZT's. The piezoelectric loss increases in general with vibration velocity.

However, the change ratio is different. The piezoelectric loss increased by a very small factor for the hard PZT (20% per 0.1 m/s) than the soft PZT (70% per 0.1 m/s), which is one order of magnitude larger than the dielectric and elastic loss variation rates. It is important to note that the piezoelectric loss $\tan \theta'$ increases almost linearly with vibration velocity, but there seems to be two steps in the change in mechanical loss $\tan \phi'$ in the case of hard PZT: almost constant up to 0.13 m/s, and followed by the rate of 75% per 0.1 m/s, similar rate to the soft PZT. This reason is under consideration from the domain dynamics viewpoint.

8 | HIGH-POWER MEASUREMENT UNDER DC BIAS FIELD

High-power measurements were conducted under externally applied DC bias field using the burst mode. Because the

open-circuit burst drive was not available (external DC bias effect cannot be measured), only the short-circuit (under a constant E_{bias}) burst drive could be achieved. The elastic compliance, as well as the elastic loss for both samples were measured as a function of vibration velocities at various levels of externally applied DC bias field. Figure 6 shows respective graphs demonstrating the variation in the elastic properties and the elastic loss $\tan \phi'$ for the hard and soft PZT's. Positive DC bias field provided a decrease in both elastic compliance and loss. The % elastic loss decrease per 100 V/mm was noted to be -2.5% for the hard PZT, whereas -3.0% for the soft PZT under 0.03 m/s, which significantly increased -3.5% for the hard and -4.2% for the soft under 0.3 m/s. More precisely, the decrease rate is enhanced as the vibration velocity is increased for both the hard and soft PZT's. The elastic compliance increased with the rate of 2.9% for the hard PZT and 4.8% per 0.1 m/s for the soft PZT at a small DC

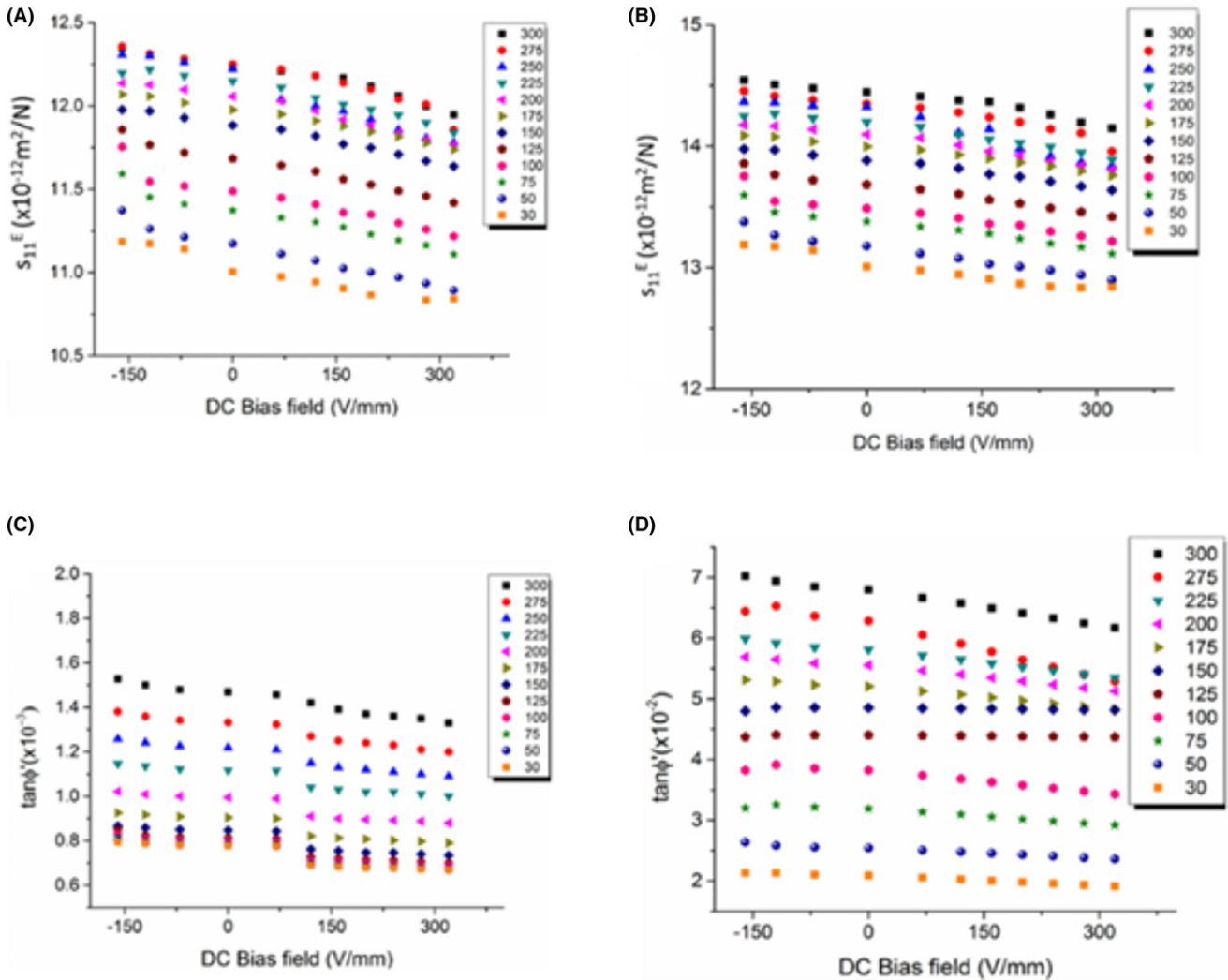


FIGURE 6 Elastic properties for PZT's at high-power conditions under DC bias (A) Elastic compliance for PIC 144 (hard PZT) (B) Elastic compliance for PIC 255 (soft PZT) (C) Elastic loss for PIC 144 (hard PZT) (D) Elastic loss for PIC 255 (soft PZT)

bias field of 50 V/mm., whereas, as the DC bias field was increased to 300 V/mm, the % decrease in elastic compliance per 0.1 m/s was -0.7% for the hard PZT and -1.7% for the soft PZT. The % elastic loss decrease per 100 V/mm was noted to be -2.5% for the hard PZT, whereas -3.0% for the soft PZT under 0.03 m/s, which are significantly enhanced to -3.5% for the hard and -4.2% for the soft under 0.3 m/s.

Likewise, it turns out to be essential to consider that negative DC bias field gives very nearly an equivalent and inverse change in the change in properties. It means that both elastic compliance and loss decreases with positive DC bias field which is just exactly opposite to the effect of negative DC Bias field. In conclusion, the external DC bias field stabilizes the high-power vibration excitation in the case of a positive bias field and destabilizes in the case of a negative bias field. Regarding the antiresonance measurement for determining the piezoelectric and dielectric losses, we will report an alternative way in successive papers.

9 | LOW-POWER MEASUREMENTS UNDER EXTERNAL DC BIAS FIELD

Although the low-power measurements under external DC bias field have been reported by several researchers,^{14,20} we performed similar experiments on the hard and soft PZT's to perform a comparative study between low- and high-power measurements. The experiments were performed using continuous admittance spectrum method. Since the vibration velocity was less than 0.030 m/s, we did not observe the heat generation more than 1°C even at the resonance frequency range for both hard and soft PZT's.

10 | DIELECTRIC PERMITTIVITY AND DIELECTRIC LOSS

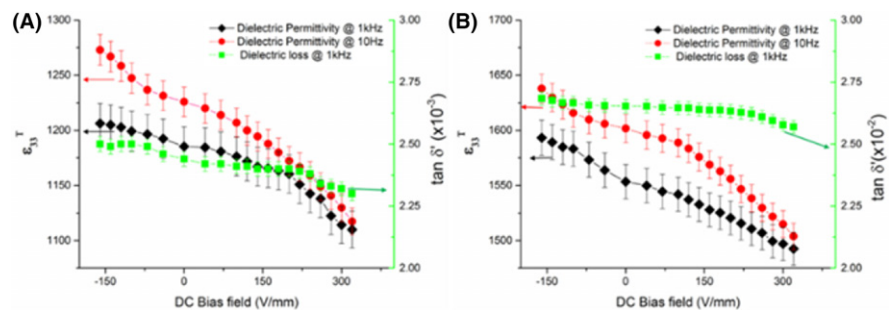
Figure 7A,B show the dielectric permittivity and dielectric loss measured with the LCR meter at an off-resonance frequency of 1 kHz (much lower than the resonance frequency ~ 40 kHz). Note that we reported earlier in the

paper that the dielectric permittivity at the resonance was slightly lower than the off-resonance. As it can be seen from Figure 7, the dielectric constant change was -0.8% for the hard PZT and -1.7% per 100 V/mm for the soft PZT for a positive bias field and 0.5% for hard PZT and 1.2% for soft PZT in the case of a negative bias field. As a reference, permittivity at 10 Hz as a function of DC bias field is plotted, calculated from the derivative of the P - E hysteresis curve shown in Figure 2. The dielectric permittivity at 10 Hz is larger than that at 1 kHz in both the hard and soft PZT's, which mainly caused by the different measuring methods, but a frequency dependency of the permittivity cannot be excluded now. In this low-frequency permittivity, however, a steeper bend seems to happen around 200 and 100 V/mm for the hard and soft PZT's in the case of positive bias field, which may indicate a sort of threshold of the domain wall dynamics, suggesting a two-step mechanism. The intensive dielectric loss $\tan \delta'$ (note one order of magnitude difference between the hard and soft PZT's) shows a decreasing tendency with a positive DC bias field with a similar bend around 200 V/mm and an increasing tendency with a negative DC bias field. Although both samples did not exhibit significant dielectric loss change, the change rate (-0.4% per 100 V/mm) of the hard PZT is less than the rate (-1.5% per 100 V/mm) of the soft PZT for a positive DC bias field.

11 | ELASTIC COMPLIANCE AND ELASTIC LOSS

Admittance spectrum method was adopted for measuring low-power properties under an external electric field. The % change in elastic compliance was -0.7% per 100 V/mm for the hard PZT, in comparison to -1.7% for the soft PZT for positive bias field and 0.5% for hard PZT and 1.4% for soft PZT in the case of negative bias field. The elastic compliance decrease with the positive DC bias field indicates that the PZT ceramics gets hardened as the DC Bias field is applied, whereas effect of negative DC bias field is completely opposite. The elastic loss (inverse of the mechanical quality factor as shown in Figure S4) showed a

FIGURE 7 Dielectric permittivity and the corresponding loss at 1 kHz frequency for (A) PIC 144 (hard PZT) (B) PIC 255 (soft PZT). Dielectric permittivity and loss decreases with applied DC bias field



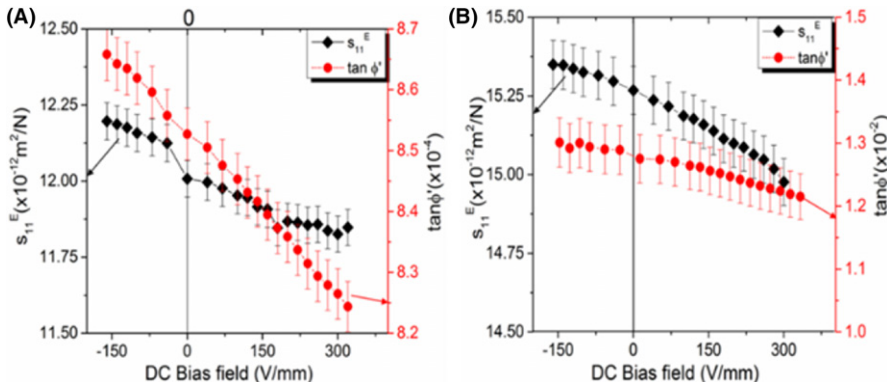


FIGURE 8 Elastic compliance and the corresponding loss for (A) PIC 144 (hard PZT) (B) PIC 255 (soft PZT)

shift of -1.1% per 100 V/mm for the hard PZT and -2.4% for soft PZT with increasing positive DC Bias field. Also, it showed a shift of 0.8% per 100 V/mm for the hard PZT and 1.9% for the soft PZT under negative DC bias field as inserted in Figure 8.

12 | PIEZOELECTRIC CONSTANT AND PIEZOELECTRIC LOSS

In addition to the quality factor Q_A at the resonance condition, mechanical quality factor Q_B was also measured at the anti-resonance condition under DC bias field (as shown in Figure S4). Thus, the piezoelectric constant and loss were determined from Equation (5) as a function of the DC bias field (Figure 9). The piezoelectric constant decrease for the hard PZT (-1% per 100 V/mm) was less than for the soft PZT (-1.5% per 100 V/mm) under a positive DC bias field. Also, apart from the real parameter, piezoelectric loss change in the hard PZT was again smaller (-1.9% per 100 V/mm) for the hard PZT as compared with the soft PZT (-3.1%). For negative DC bias field, the piezoelectric constant increase for the hard PZT (0.7% per 100 V/mm) was less than for the soft PZT (1.2% per 100 V/mm). Apart from that, piezoelectric loss change in the hard PZT was again smaller (1.5% per 100 V/mm) as compared with the soft PZT (2.8% per 100 V/mm). Also, it has been shown here that piezoelectric constant as well as piezoelectric loss decreases with positive DC bias field which is just exactly opposite to the effect of negative DC Bias field.

13 | SUMMARY

In this paper, we provided the dependency of dielectric, elastic and piezoelectric coefficients (real parameters and imaginary losses) on the vibration velocity and DC bias field comprehensively. Note that as we drive the piezoelectric ceramic at a high vibration velocity, we are introducing AC stress in the material. Table 1 summarizes the material's

coefficients change with the vibration velocity and DC electric field. Note that our results are not associated with any temperature rise during the measurements. It has been found that with the vibration velocity increase, the dielectric constant, elastic compliance, piezoelectric coefficient, and their corresponding losses increase for both the hard and soft PZT's. However, the change is more pronounced in the soft PZT as compared with the hard PZT. To the contrary the influence of a DC bias field depends strongly of the direction of the field with respect to the original poling field. A net decrease in the dielectric constant, elastic compliance, piezoelectric coefficient and their corresponding losses is observed when a positive DC Bias field is applied, whereas a negative DC bias field affects in a completely opposite way. The decrease rate of these physical parameters under small vibration level is enhanced under large vibration level, as shown in the third column in Table 1. This situation can be visualized in the 3D plot in Figure 10, showing the dependence of elastic loss $\tan \phi'$ on the externally applied DC bias field and the vibration velocity at the k_{31} sample length edge in the hard (PIC 144) and soft (PIC 255) PZT. In comparison with a relatively smooth plane contour for the soft PZT, a clear bend on the contour plane is observed for the hard PZT. We can find the intensive elastic loss $\tan \phi'$ shows two different trends under vibration velocity and DC bias field; increasing with the vibration velocity (domain wall destabilization) and decreasing with positive DC bias field (domain wall stabilization). Roughly speaking, the vibration velocity 0.1 m/s ($+3\%$ and 5% change in s_{11}^E for the hard and soft PZT's) exhibits the almost equivalent "opposite" change rate ($-1.7\% \times 2$ and $-2.3\% \times 2$ changes in s_{11}^E for the hard and soft PZT's) of 200 V/mm DC electric field.

This equivalency can be understood roughly as follows. Like the off-resonance analysis in Ref. 20, the external stress X_1 is roughly estimated with the external electric field E_3 by

$$X_1 = (d_{31}/s_{11}^E)E_3 \quad (14)$$

Conversely, the electric field induced by the stress is estimated by

FIGURE 9 Piezoelectric constant and the corresponding loss for (A) PIC 144 (hard PZT) (B) PIC 255 (soft PZT)

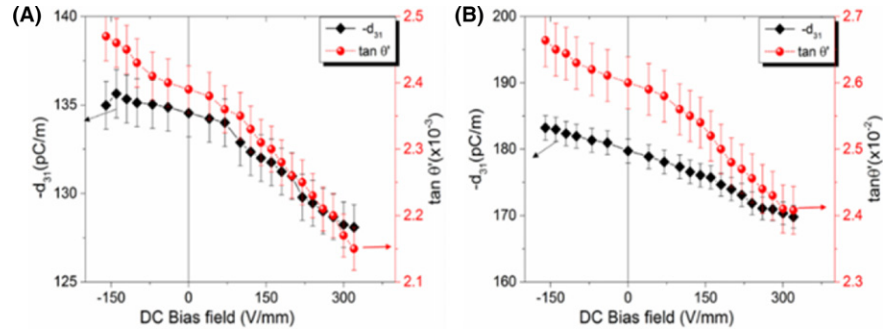
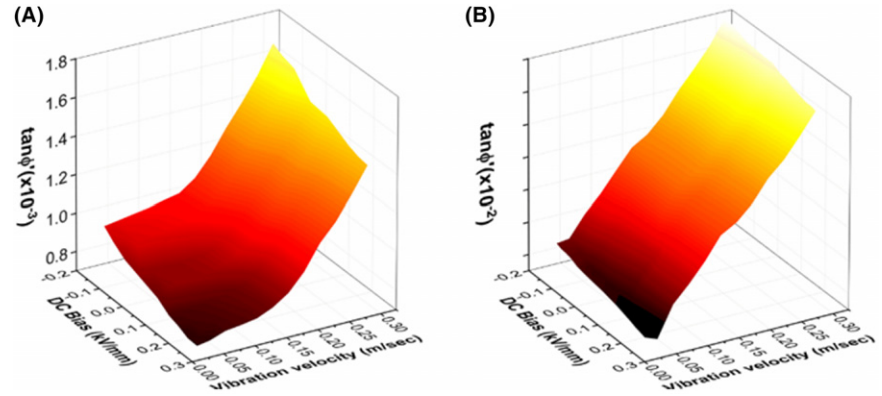


TABLE 1 Table showing net change in material properties with applied positive DC bias field and vibration velocity

% Change in material properties	Vibration velocity (per 0.1 m/s)		Electric field (per 100 V/mm at 0.01 m/s)		Electric field (per 100 V/mm at 0.3 m/s)	
	Hard PZT (%)	Soft PZT (%)	Hard PZT (%)	Soft PZT (%)	Hard PZT (%)	Soft PZT (%)
Dielectric constant (ϵ_{33}^T)	+2.9	+5	-0.8	-1.7	-	-
$\tan \delta_{33}'$	-	-	-0.4	-1.5	-	-
Elastic compliance (s_{11}^E)	+3	+5	-0.7	-1.7	-1.7	-2.3
$\tan \phi_{11}'$	+75	(+)-0 & 75	-1.1	-2.4	-3.5	-4.2
Piezoelectric constant (d_{31})	+2.7	+5.1	-1	-1.5	-	-
$\tan \theta_{31}'$	+70	+20	-1.9	-3.1	-	-
Electromechanical coupling factor (k_{31})	+3.5	+5.3	Change within error limits	Change within error limits	-	-

FIGURE 10 3D plot showing the variation of elastic loss for PZT's as a function of DC Bias field and vibration velocity for (A) PIC 144 (hard PZT) (B) PIC 255 (soft PZT)



$$E_3 = (d_{31}/\epsilon_0\epsilon_{33}^X)X_1. \quad (\text{or } X_1 = (\epsilon_0\epsilon_{33}^X/d_{31})E_3) \quad (15)$$

Since the electromechanical coupling factor $\frac{d_{31}}{\sqrt{\epsilon_0\epsilon_{33}^X s_{11}^E}}$ is not equal to 1, $d_{31}/s_{11}^E \neq \epsilon_0\epsilon_{33}^X/d_{31}$. Thus, we adopt a geometric average relationship for evaluating X_1 :

$$X_1 = -\sqrt{\frac{\epsilon_0\epsilon_{33}^X}{s_{11}^E}}E_3 \quad (16)$$

The sign “-” stands for the opposite effect owing to the transversal piezoelectric effect (i.e., $d_{31} < 0$). We may extend this relationship at the resonance by multiplying the mechanical quality factor Q_m :

$$|X_1| = Q_m \sqrt{\frac{\epsilon_0\epsilon_{33}^X}{s_{11}^E}}|E_3| \quad (17)$$

Using practical values for the hard PZT ($(s_{11}^E = 12 \times 10^{-12}$, $\epsilon_{33}^X = 1100$ and $Q_m = 1200)$ and $E_3 = 200$ V/mm, X_1 becomes 6.8×10^6 N/m². On the other hand, the relation between the maximum $X_{1,rms}$ (at the k_{31} plate sample center) and vibration velocity $v_{1,rms}$ (at the sample edge) is given by¹⁹

$$X_{1,rms} = \sqrt{\frac{\rho}{s_{11}^E}}v_{1,rms} \quad (18)$$

Using practical values for the hard PZT ($\rho = 7.5 \times 10^3$ and $s_{11}^E = 12 \times 10^{-12}$) again, $v_{1,rms} = 0.1$ m/s provides X_1 ,

$\sigma_{rms} = 2.5 \times 10^6 \text{ N/m}^2$ or $X_{1,peak} = 4.0 \times 10^6 \text{ N/m}^2$, which shows a reasonable agreement (in the same order) with the value estimated by Equation (16).

Another noteworthy point is the two-step mechanism observed in Figures 5, 7 and 10 in the hard PZT: a change in gradient can be observed in the elastic loss $\tan \phi'$ on the vibration velocity change, whereas a change in the gradient of dielectric constant ϵ_{33}^X and dielectric loss $\tan \delta'$ is observed on the DC bias field change. This may suggest a sort of threshold value in terms of mechanical stress or electrical field in the hard PZT for stabilizing/destabilizing the domain wall motions. This could be related to domain stabilization threshold, and the detailed analysis of the results will be reported in future papers.

ACKNOWLEDGMENT

This work was supported by Office of Naval Research under Grant No. N00014-14-1-1044. Also, the authors thank Minkyu Choi for useful and helpful discussions during the entire work.

ORCID

Anushka Bansal  <http://orcid.org/0000-0003-4340-362X>

REFERENCES

1. Wallaschek J. Piezoelectric ultrasonic motors. *J Intell Mater Syst Struct.* 1995;6:71-83.
2. Uchino K. Materials issues in design and performance of piezoelectric actuators: an overview. *Acta Mater.* 1998;46:3745-3753.
3. Damjanovic D. Materials for high temperature piezoelectric transducers. *Curr Opin Solid State Mater Sci.* 1998;3:469-473.
4. Miyake S, Morita T. Piezoelectric nonlinearity and its temperature dependency under high power driving. *Precision Engineering Society Academic Lecture Papers Proceedings Spring meeting of Precision Engineering Society of Japan Corporation.* 2016;3-4.
5. Priya S, Viehland D, Carazo AV, et al. High-power resonant measurements of piezoelectric materials: importance of elastic nonlinearities. *J Appl Phys.* 2001;90:1469-1479.
6. Hall DA. Nonlinearity in piezoelectric ceramics. *J Mater Sci.* 2001;36:4575-4601.
7. Adachi K, Ogasawara I, Tamura Y, et al. Influence of static prestress on the characteristics of bolt-clamped Langevin-type transducers. *Jpn J Appl Phys.* 1998;37:2982-2987.
8. Transducer BL, Takahashi T, Adachi K. Influence of static prestress on the characteristics of bolt-clamped Langevin-type transducers". *Jpn J Appl Phys.* 1998;1998(37):2982-2987.
9. Adachi K, Konno Y, Masaki S. Development of bolt-clamped Langevin-type transducer factor for excitation of large torsional vibration with high mechanical quality. *Jpn J Appl Phys.* 1994;33: 1182-1188.

10. Gao Y, Uchino K, Viehland D. Domain wall release in 'hard' piezoelectric under continuous large amplitude ac excitation. *J Appl Phys.* 2007;101:71-83.
11. Gao J, Hu X, Zhang L, et al. Major contributor to the large piezoelectric response in $(1-x)\text{Ba}(\text{Zr}_{0.2}\text{Ti}_{0.8})\text{O}_3x(\text{Ba}_{0.7}\text{Ca}_{0.3})\text{TiO}_3$ ceramics: domain wall motion. *Appl Phys Lett.* 2014;104:252.
12. Gao Y, Uchino K, Viehland D. Time dependence of the mechanical quality factor in 'hard' lead zirconate titanate ceramics: development of an internal dipolar field and high power origin. *Jpn J Appl Phys.* 2006;45:9119-9124.
13. Uchino K, Negishi H, Hirose T. Drive voltage dependence of electromechanical resonance in PLZT piezoelectric ceramics. *Jpn J Appl Phys.* 1989;28:47-49.
14. Wang QM, Zhang T, Chen Q, et al. Effect of DC bias field on the complex materials coefficients of piezoelectric resonators. *Sens Actuators A Phys.* 2003;109:149-155.
15. Shekhani H, Scholehwar T, Hennig E, et al. Characterization of piezoelectric ceramics using the burst/transient method with resonance and antiresonance analysis. *J Am Ceram Soc.* 2016;10:1-10.
16. Shekhani HN, Gurdal EA, Ural SO, et al. Analysis of High Power Behavior in Piezoelectric Ceramics from a Mechanical Energy Density Perspective. arXiv:1605.06685.
17. Ural SO, Tuncdemir S, Zhuang Y, et al. Development of a high power piezoelectric characterization system and its application for resonance/antiresonance mode characterization. *Jpn J Appl Phys.* 2009;48:5091-5095.
18. Uchino K, Hirose S. Loss mechanisms in piezoelectrics: how to measure different losses separately. *IEEE Trans Ultrason Ferroelectr Freq Control.* 2001;48:307-321.
19. Shekhani HN, Uchino K. Characterization of mechanical loss in piezoelectric materials using temperature and vibration measurements. *J Am Ceram Soc.* 2014;97:2810-2814.
20. Masys AJ, Ren W, Yang G, et al. Piezoelectric strain in lead zirconate titanate ceramics as a function of electric field, frequency, and dc bias. *J Appl Phys.* 2015;94:1155-1162.
21. Blackburn JF, Cain MG. Non-linear piezoelectric resonance analysis using burst mode: a rigorous. *J Phys D Appl Phys.* 2007;40: 227-233.
22. Lyon. Non linearities in Langevin transducers. 1994; 925-928.
23. B. S. Institution and C. (Organization), Piezoelectric properties of ceramic materials and components, no. pt. 3. BSI. 2002.

SUPPORTING INFORMATION

Additional Supporting Information may be found online in the supporting information tab for this article.

How to cite this article: Bansal A, Shekhani HN, Majzoubi M, Hennig E, Scholehwar T, Uchino K. Improving high-power properties of PZT ceramics by external DC bias field. *J Am Ceram Soc.* 2018;00: 1–10. <https://doi.org/10.1111/jace.15437>